Large uncertainty in carbon uptake potential of land-based climate-change mitigation efforts

Krause, Andreas; Pugh, Thomas; Bayer, Anita; Li, Wei; Leung, Felix; Bondeau, Alberte; Doelman, Jonathan C.; Humpenöder, Florian; Anthoni, Peter; Bodirsky, Benjamin; Ciais, Philippe; Müller, Christoph; Murray-Tortarolo, Guillermo; Olin, Stefan; Popp, Alexander; Sitch, Stephen; Stehfest, Elke; Arneth, Almut

Document Version
Peer reviewed version

[Link to publication on Research at Birmingham portal](#)

1 **Title page**

2 Title: Large uncertainty in carbon uptake potential of land-based climate-change mitigation

3 efforts

4 Running head: Large uncertainty in carbon uptake potential

5 List of authors: Andreas Krause[1], Thomas A. M. Pugh[1,2], Anita D. Bayer[1], Wei Li[3], Felix

6 Leung[4], Alberte Bondeau[5], Jonathan C. Doelman[6], Florian Humpenöder[7], Peter Anthoni[1],

7 Benjamin L. Bodirsky[7], Philippe Ciais[3], Christoph Müller[7], Guillermo Murray-Tortarolo[4],

8 Stefan Olin[8], Alexander Popp[7], Stephen Sitch[4], Elke Stehfest[6], Almut Arneth[1]

9 Institute or laboratory of origin: [1]Karlsruhe Institute of Technology, Institute of Meteorology

10 and Climate Research – Atmospheric Environmental Research (IMK-IFU), Kreuzeckbahnstr.

11 19, 82467 Garmisch-Partenkirchen, Germany

12 [2]School of Geography, Earth & Environmental Sciences and Birmingham Institute of Forest

13 Research, University of Birmingham, B15 2TT, United Kingdom

14 [3]Laboratoire des Sciences du Climat et l'Environnement, CEA-CNRS-UVSQ, Gif-sur-Yvette,

15 France

16 [4]College of Life and Environmental Sciences, University of Exeter, Exeter, United Kingdom

17 [5]Institut Méditerranéen de Biodiversité et d'Ecologie marine et continentale (Mediterranean

18 Institute for Biodiversity and Ecology, IMBE), Aix-en-Provence, France

19 [6]Department of Climate, Air and Energy, Netherlands Environmental Assessment Agency

20 (PBL), PO Box 30314, 2500 GH The Hague, Netherlands

21 [7]Potsdam Institute for Climate Impact Research (PIK), Telegrafenberg, PO Box 60 12 03,

22 14412 Potsdam, Germany

23 [8]Department of Physical Geography and Ecosystem Science, Lund University, 22362 Lund,

24 Sweden

25 Corresponding author's telephone and email details: ++49 8821 183186,

26 andreas.krause@kit.edu

29 Paper type: Primary Research Article

30

31 **Abstract**

32 Most climate mitigation scenarios involve negative emissions, especially those that aim to

33 limit global temperature increase to 2°C or less. However, the carbon uptake potential in land-

34 based climate change mitigation efforts is highly uncertain. Here, we address this uncertainty

35 by using two land-based mitigation scenarios from two land-use models (IMAGE and

36 MAgPIE) as input to four dynamic global vegetation models (DGVMs; LPJ-GUESS,

37 ORCHIDEE, JULES, LPJmL). Each of the four combinations of land-use models and

38 mitigation scenarios aimed for a cumulative carbon uptake of ~130 GtC by the end of the

39 century, achieved either via the cultivation of bioenergy crops combined with carbon capture

40 and storage (BECCS) or avoided deforestation and afforestation (ADAFF).

41 Results suggest large uncertainty in simulated future land demand and carbon uptake rates,

42 depending on the assumptions related to land use and land management in the models. Total

43 cumulative carbon uptake in the DGVMs is highly variable across mitigation scenarios,

44 ranging between 19 and 130 GtC by year 2099. Only one out of the 16 combinations of

45 mitigation scenarios and DGVMs achieves an equivalent or higher carbon uptake than

46 achieved in the land-use models. The large differences in carbon uptake between the DGVMs

47 and their discrepancy against the carbon uptake in IMAGE and MAgPIE are mainly due to

48   different model assumptions regarding bioenergy crop yields, and due to the simulation of soil

49   carbon response to land-use change. Differences between land-use models and DGVMs

50   regarding forest biomass and the rate of forest regrowth also have an impact, albeit smaller,

51   on the results. Given the low confidence in simulated carbon uptake for a given land-based

52   mitigation scenario, and that negative emissions simulated by the DGVMs are typically lower

53   than assumed in scenarios consistent with the 2°C target, relying on negative emissions to

54   mitigate climate change is a highly uncertain strategy.

55

Introduction

57   "Negative emissions", i.e. the removal of carbon dioxide (CDR) from the atmosphere, is an

58   important concept for climate change mitigation (Lenton and Vaughan, 2009). Scenarios

59   based on land-use (LU) models or Integrated Assessment Models (IAMs) tend to achieve an

60   end-of-century warming goal at or below 2°C only through negative emissions which

61   commence within the next 1-2 decades, and then increase and are sustained at considerable

62   rates during the second half of the 21st century (Anderson and Peters, 2016, Fuss *et al.*, 2014,

63   Gasser *et al.*, 2015, Riahi *et al.*, 2017, Rogelj *et al.*, 2015, Sanderson *et al.*, 2016, Smith *et al.*,

64   2016a). So far, negative emissions represented in IAMs are mainly land-based options (Popp

65   *et al.*, 2017, Popp *et al.*, 2014b).

66   IAMs currently focus on two land-based CDR technologies which both utilize the carbon (C)

67   uptake by plants via photosynthesis. One is large-scale cultivation of crops or trees for

68   bioenergy and capturing the C released upon combustion for long-term storage in geologic

69   formations (BECCS). The other is to maintain or increase terrestrial C stocks via avoided

70   deforestation and afforestation/reforestation (ADAFF). These are the two most widely-used

71   options in IAMs to achieve negative emissions because they do not have to rely on the

72 development of new, large-scale technology (ADAFF), or are regarded as the most prolific

73 option with the capability to supply energy (BECCS) (Humpenöder *et al.*, 2014, Smith *et al.*,

74 2016a). However, the land demand/availability of these approaches is highly uncertain

75 (Boysen *et al.*, 2017a, Popp *et al.*, 2017), and their potential to remove significant amounts of

76 C from the atmosphere is regarded as controversial (Fuss *et al.*, 2014). Additionally, conflicts

77 with other LU, associated supply of ecosystem services, and maintenance/enhancement of

78 biodiversity are highly likely (Krause *et al.*, 2017, Smith *et al.*, 2016a, Williamson, 2016).

79 Considering typical time frames of decades involved in the planning and establishment of

80 climate mitigation projects, the quantification of their uncertainties in terms of achievable

81 CDR is important to inform policy makers about practicality and risks.

82 Here, we address the uncertainty of C uptake potential from land-based climate change

83 mitigation by using projections of future land-use change (LUC) from one IAM (IMAGE)

84 and one socio-economic LU model (MAgPIE; for simplicity we refer to IMAGE and

85 MAgPIE as land-use models - LUMs - in the following) as input to four dynamic global

86 vegetation models (DGVMs; LPJ-GUESS, ORCHIDEE, JULES, LPJmL). In these scenarios,

87 C uptake is achieved either via BECCS or via ADAFF. The cumulative additional C uptake

88 target in each mitigation LUC scenario is 130 GtC by year 2100 compared to a baseline LUC

89 scenario without additional land-based mitigation (BASE). We analyze total C uptake and the

90 relative contribution of vegetation, soils, and C storage via CCS in the four DGVMs and

91 compare it to the C uptake targeted and achieved in the LUMs.

92

93 **Materials and methods**

94 Detailed information about the LUMs and the scenarios can be found in Krause et al. (2017).

95 In the following we provide a short description of the LUMs and the scenarios.

96

97   Description of the land-use models

98   The Integrated Model to Assess the Global Environment (IMAGE) is an ecological-
99   environmental model framework simulating the environmental consequences of human
100   activities worldwide (Stehfest et al., 2014).

101   The Model of Agricultural Production and its Impact on the Environment (MAgPIE) is a
102   global LU and agro-food system model. It optimizes spatial-explicit LU patterns and
103   intensification levels to satisfy a given food, feed, material, and bioenergy demand at minimal
104   production costs (Lotze-Campen *et al.*, 2008, Popp *et al.*, 2014a).

105   Climate change and CO_2 impacts on forest growth and crop yields are accounted for in the
106   LUMs. The LPJmL DGVM (Bondeau *et al.*, 2007) represents the crop/vegetation sub-model
107   in both IMAGE (where it is dynamically coupled) and MAgPIE (where it provides potential C
108   stocks, crop yields, irrigation water requirements, and blue water availability as input data).
109   We also use an offline version of LPJmL as one of our four DGVMs which differs from the
110   versions used in the LUMs mainly by not considering technological yield increases in the
111   future.

112

113   Land-use scenarios

114   Both LUMs harmonized their pasture and cropland LU patterns to the HYDE 3.1 dataset
115   (Klein Goldewijk *et al.*, 2011) in the years 2005 (IMAGE) or 1995 (MAgPIE) to create a
116   continuous historical-to-future time series. The simulation period was 1970-2100 for IMAGE
117   and 1995-2100 for MAgPIE, with LUC scenarios starting to diverge in year 2005. The spin-
118   up in IMAGE was set to 700 years with natural vegetation cover followed by 300 years with

119   year 1970 land-cover map, climate and CO_2. In MAgPIE, potential C densities from LPJmL

120   were used as initial (1995) values, with agricultural vegetation and litter C set to zero and soil

121   C depleted based on IPCC recommendations to account for real land cover at the start of the

122   simulation period (Humpenöder *et al.*, 2014). Socioeconomic developments as input to the

123   LUMs were based on SSP2 (Popp *et al.*, 2017). Food production in the mitigation scenarios

124   was maintained on the same levels as in BASE.

125   With respect to the rate of forest regrowth in the ADAFF scenarios, MAgPIE parameterizes

126   managed afforestation by climate region specific S-shaped growth curves towards potential

127   forest biomass, and litter and soil C recovering within 20 years (Humpenöder *et al.*, 2014). In

128   contrast, forest regrowth in IMAGE is dynamically simulated by LPJmL, which is a sub-

129   component of IMAGE. This means that similar C uptake rates following afforestation are to

130   be expected for IMAGE and the stand-alone LPJmL DGVM. Forest regrowth in IMAGE

131   partly takes place on degraded forest lands, which are assumed to be completely deforested

132   (Doelman et al., 2018).

133   The degraded forest land-cover class was implemented in IMAGE due to a mismatch between

134   deforestation   rates   reported   by   the   FAO's   2015   Forest   Resource   Assessment

135   (http://www.fao.org/3/a-i4793e.pdf, last accessed September 2017) and historical expansions

136   of cropland and pasture area reported by FAO. These differences are assumed to be caused by

137   additional reasons (e.g. unsustainable forestry preventing regrowth of natural forests, mining,

138   or illegal logging) and accounted for by a historically calibrated rate of forest degradation,

139   which is extrapolated into the future (Doelman *et al.*, 2018).

140

141   Description of the Dynamic Global Vegetation Models

142   The LUC scenarios were used as input to four DGVMs: LPJ-GUESS (Olin *et al.*, 2015, Smith

143   *et al.*, 2014), ORCHIDEE (Krinner et al., 2005), JULES (Best *et al.*, 2011, Clark *et al.*, 2011),

144   and LPJmL (Bondeau *et al.*, 2007, Sitch *et al.*, 2003). The models have different heritages;

145   while ORCHIDEE and JULES were developed as land components of global climate models

146   (IPSL and UKESM), LPJ-GUESS and LPJmL were originally designed as stand-alone offline

147   models to simulate vegetation dynamics and associated C and water fluxes. All DGVMs

148   represent vegetation using a number of plant functional types (PFTs), with LPJ-GUESS and

149   LPJmL also representing dedicated crop PFTs. LPJ-GUESS is different from the other

150   DGVMs by its explicit representation of forest demography and by having nitrogen cycling as

151   an additional constraint on ecosystem C processes (in addition to soil water availability which

152   is accounted for in all DGVMs). All DGVMs represent LUC and land management explicitly

153   even though the models differ in terms of implemented processes and level of detail. Table 1

154   and the extended Table S1 provide an overview of model differences which are important for

155   this study.

156

157   Simulation setup

158   The DGVM simulation period was 1901-2099. DGVMs were first spun up to pre-industrial

159   equilibrium state (1901), recycling 1950-1959 climatology to attain a stable equilibrium of C

160   pools and fluxes in each model using atmospheric CO_2 concentration from 1901

161   (Meinshausen et al., 2011). Climate from the 1950-1959 period was used for the spin-up

162   because these were the first years in the climate data set, a common practice in this kind of

163   set-up. DGVMs were then applied over the transient period 1901-2099 using transient CO_2

164   (Meinshausen *et al.*, 2011) and climate data (1950-2099) simulated by the IPSL-CM5A-LR

165   climate model for the representative concentration pathway RCP2.6 from the ISI-MIP project,

166   bias-corrected as in Hempel et al. (2013). The temperature increase is 2°C by the end of the

167   21st century relative to the pre-industrial era. The climate data for the spin-up and the 1901-

168   1949 period were randomly taken from the 1950-1959 period. Future atmospheric CO_2

169   mixing ratio followed the RCP2.6 pathway, peaking at 443 ppmv in year 2052 (Meinshausen

170   *et al.*, 2011). LUC was based on spatially explicit LU maps derived from the LUMs (for the

171   historic period based on HYDE3.1) and translated into the vegetation types of each DGVM

172   (see Table 1). The DGVMs aimed to be as consistent as possible with the LUMs when

173   implementing LU patterns from the LUM scenarios, e.g. for IMAGE scenarios all DGVMs

174   apart from JULES followed the IMAGE assumption of degraded forests being grasslands.

175   Management information (crop types, irrigation, and nitrogen fertilizers) were also provided

176   by the LUMs but were only used by some DGVMs which represented the relevant processes

177   explicitly (Table 1). LPJ-GUESS was the only model being able to use nitrogen fertilizers as

178   provided by the LUMs. Nitrogen application rates (synthetic plus manure) were available

179   from 1970/1995 on. They were derived to match assumed crop yields in the LUMs. A historic

180   hindcast (1901-1969/1901-1994) was calculated based on initial (1970/1995) fertilizer rates

181   from the LUMs and relative changes in the Land-Use Harmonization data set

182   (http://luh.umd.edu/index.shtml, see also Krause et al., 2017). The implementation of the LU

183   data into the DGVMs (e.g. mapping to DGVM vegetation types and defining rules by which

184   managed land expands over natural vegetation), land masks, and additional required input

185   variables (e.g. soil characteristics) were left to the responsibility of the individual DGVM

186   groups. Different model structures and implementations of the LU patterns can result e.g. in

187   differences in global forest area in the individual DGVMs (Fig. S1). The spatial resolution of

188   the DGVMs was the same as the resolution of the input data (0.5°x0.5°), except for

189   ORCHIDEE (2°x2°). In total, 24 combinations of DGVMs and LUC scenarios were

190   simulated, including 16 combinations of DGVMs and mitigation LUC scenarios.

191

Results

Land-use scenarios

In both LUMs, LUC is generally greater for ADAFF scenarios than for BECCS scenarios (Fig. S2) because the former is simulated with LUMs to be less efficient at CDR than the latter (Humpenöder, et al., 2014). The different C accumulation trajectories in ADAFF (see methods) result in ADAFF activities starting earlier in IMAGE but avoided deforestation/afforestation area being slightly larger in MAgPIE by the end of the century (Figs. S1, S2a,b, Table S2). Forest area by year 2099 is 1040 Mha larger in ADAFF than in BASE for IMAGE and 1103 Mha larger for MAgPIE. For IMAGE, ~42% of this difference in forest area can be attributed to avoided deforestation and 58% to afforestation. For MAgPIE, the corresponding numbers are only 4% for avoided deforestation and 96% for afforestation, emphasizing the much larger role of afforestation compared to avoided deforestation in MAgPIE. The LUMs also differ in terms of land-cover classes affected by ADAFF activities. In IMAGE, forest maintenance and expansion usually takes place on pastures or degraded forests (ADAFF compared to BASE), but in MAgPIE afforestation on abandoned croplands is also relevant, particularly after year 2070 (see Table S2; note that some of the abandoned cropland in MAgPIE ADAFF is not afforested but instead converted to pasture while at other locations pastures are converted to forests, resulting in small net changes in pasture area by the end of the century).

The area needed for bioenergy production is mainly taken from natural vegetation in IMAGE but also from existing agricultural land in MAgPIE. IMAGE has a larger bioenergy land demand to fulfil the same CCS target as MAgPIE (Fig. S2c,d). This reflects different modelling approaches: in IMAGE, land allocation for bioenergy cultivation follows a rule-

215   based approach according to sustainability criteria, implying that only marginal land not

216   needed for food production is available for bioenergy. In MAgPIE, bioenergy and food

217   production compete for fertile land based on a cost minimization procedure. Consequently,

218   average bioenergy yields are lower in IMAGE than in MAgPIE, thereby increasing the

219   required area to deliver the same annual CCS rates.

220

221   Present-day carbon pools and future changes in the baseline scenarios

222   Present-day C pools as simulated by IMAGE and MAgPIE are 440 and 484 GtC in global

223   vegetation, and 1121 and 1981 GtC in the soils (including litter), respectively. The large

224   divergence in soil C between the two LUMs is likely mainly due to the representation of

225   permafrost in MAgPIE. Vegetation C simulated by the DGVMs ranges between 275 and 425

226   GtC, and soil C between 1315 and 1954 GtC (Fig. S3). For the two non-mitigation BASE

227   scenarios, in all DGVMs except LPJmL the land acts as a net C sink between year 2000 and

228   2099 (Fig. S3). The magnitude and direction of change in C pools is determined by the

229   DGVM's response to RCP2.6 climate change, CO_2 fertilization, and baseline LUC.

230

231   Total carbon uptake in the mitigation scenarios

232   Total additional C uptake in the mitigation scenarios is here calculated as the sum of changes

233   in vegetation C, litter and soil C, and (relatively negligible) product pool C, plus cumulative

234   CCS (all relative to BASE). While an uptake target of 130 GtC was set in both LUMs, actual

235   C uptake in the LUMs in most cases deviates somewhat from this number. For the ADAFF

236   scenarios, the simplicity of the afforestation implementation in IMAGE was unable to exactly

237   meet the target. In MAgPIE, afforestation decision-making was based on present-day

238 potential C pools. Potential impacts of climate change on the terrestrial C storage capacity

239 were therefore not considered which leads to a mismatch between intended and actual

240 sequestration. The realized C uptake in ADAFF between year 2005 and 2099 is 141 GtC in

241 IMAGE and 120 GtC in MAgPIE (Figs. 1a,b, 2a). Around 49% of the total C increase in

242 IMAGE ADAFF can be attributed to avoided deforestation and 51% to afforestation (for

243 MAgPIE spatial C stocks were not available but afforestation is certainly much more

244 important due to the limited decline in forest area in MAgPIE BASE). For BECCS, in both

245 LUMs the CDR target was implemented as a gross CCS target which included the harvested

246 C from bioenergy crops and a fractional (80%; Klein et al., 2014) capture and storage of this

247 harvest. Cumulative CCS reaches 128 GtC in year 2099 in both LUMs (see subsection

248 "Cumulative CCS") so the implemented CDR/CSS target is achieved. However, calculations

249 of the target in the LUMs originally neglected terrestrial C losses from deforestation for

250 bioenergy cultivation. When these are included, cumulative CCS combined with ecosystem C

251 losses from deforestation result in a net total C uptake of 86 and 107 GtC, thus below the

252 sought target due to emissions from LUC.

253 In contrast to the two LUMs, total C uptake (relative to BASE) is typically lower in the

254 DGVM simulations forced by the same LU patterns, with total C uptake in the DGVMs

255 ranging between 19 and 130 GtC (Figs. 1a,b, 2a). Unsurprisingly (as LPJmL represents the

256 vegetation component of the LUMs), the closest agreement exists between the LUMs and

257 LPJmL. ORCHIDEE simulates the lowest uptake for ADAFF and JULES the lowest uptake

258 for BECCS. The maximum yearly total C uptake per decade within the 21st century ranges

259 from 1.9 GtC yr^{-1} (IMAGE ADAFF) to 3.5 GtC yr^{-1} (MAgPIE ADAFF) in the LUMs and

260 from 0.4 GtC yr^{-1} (ORCHIDEE IMAGE-ADAFF) to 2.0 GtC yr^{-1} (LPJmL IMAGE-BECCS)

261 in the DGVMs. Spatially, total C uptake is concentrated in the tropics for ADAFF (except in

262 ORCHIDEE, which simulates substantial emissions in some regions), while patterns are more

263   diverse for BECCS (Fig. 3). The largest agreement in total C uptake across DGVMs is found

264   in tropical Africa for the ADAFF scenarios (Fig. S4). The contributions of vegetation, soil,

265   and cumulative CCS to model discrepancies in total C uptake are analyzed in the following

266   subsections.

267

268   Vegetation carbon

269   As intended, the simulations with the ADAFF scenarios result in increasing biomass over the

270   21st century compared to the BASE simulations for all LUMs and DGVMs. Vegetation C

271   uptake in year 2099 is 79 and 66 GtC in IMAGE and MAgPIE and ranges between 39 and 73

272   GtC in the DGVMs (Figs. 1c,d, 2b), with generally larger uptake for IMAGE scenarios than

273   for MAgPIE scenarios due to the earlier start of ADAFF activities in IMAGE (Table S2).

274   Biomass accumulation occurs at a relatively steady rate in the DGVMs but accelerates during

275   the second half of the century in the LUMs (Fig. 1c,d). There is a drop in vegetation C for

276   LPJmL MAgPIE-ADAFF around mid-century. As agricultural land has low vegetation C

277   pools in LPJmL this is related to a decreasing vegetation C density in forests, which is not

278   compensated for by the simultaneous increase in forest area. Tree PFTs in LPJmL are

279   represented by average individuals (representing all trees belonging to this PFT), and the

280   individual's properties are changed when afforestation occurs in a grid-cell. These changes in

281   the PFT's properties might in some regions reduce its ability to compete or make it more

282   vulnerable to disturbances so that tree mortality is increased compared to the BASE scenario

283   in which no afforestation took place.

284   The vegetation C uptake in IMAGE can be equally attributed to avoided deforestation and to

285   afforestation (Table S3). No quantification is possible in MAgPIE because spatial C stocks

286   were not available. In the DGVMs, the contribution of avoided deforestation to the vegetation

287 C uptake in ADAFF is generally larger for IMAGE-LU than for MAgPIE-LU (Table S3),

288 confirming the much larger role of afforestation compared to avoided deforestation in

289 MAgPIE. For BECCS, all LUMs and DGVMs simulate deforestation-driven decreases in

290 vegetation C. JULES simulates the largest biomass losses upon deforestation and ORCHIDEE

291 the smallest losses. Since global vegetation C stocks are similar across DGVMs (with the

292 exception of ORCHIDEE, Fig. S3), differences in C losses arise from spatial variations in

293 biomass which DGVMs (and presumably LUMs) are known to not capture well (Johnson et

294 al., 2016). BECCS deforestation emissions are generally larger for IMAGE-LU patterns than

295 for MAgPIE-LU patterns, reflecting the much larger decline in forest area (Fig. S1, Table S2).

296 Site-level comparisons can help us to better understand differences across models. Therefore,

297 in order to understand local responses better and to use these to interpret the simulated global

298 totals, we extracted grid-cells from the global simulations (for IMAGE scenarios as spatial

299 information were not available from MAgPIE), selected because a large fraction of the grid-

300 cells' area underwent land-cover transitions within the 21st century. However, there are

301 substantial variations in the models' response to LUC across different sites, making it difficult

302 to choose representative grid-cells and to draw universal conclusions from this comparison.

303 Figure S5 shows three relatively representative example sites. As expected for a 0.5°

304 resolution, there are substantial differences on grid-cell level across models in terms of initial

305 vegetation C densities. All models simulate increasing biomass in response to afforestation

306 (Fig. S5a,b) and biomass losses upon deforestation (Fig. S5c). However, JULES does not

307 simulate forest degradation (Fig. S5c; see methods for more information about degraded

308 forests), contributing to the lower vegetation C uptake compared to the other DGVMs for the

309 IMAGE ADAFF scenario.

310 For MAgPIE scenarios, site-level comparisons are not shown because MAgPIE only reported

311 global C pools. For the MAgPIE ADAFF scenario, global vegetation C uptake is very similar

312   in all DGVMs but lower than in MAgPIE (Fig. 1d). It seems that one reason for this

313   divergence is different assumptions about potential vegetation C stocks (available for

314   MAgPIE and LPJ-GUESS; see Fig. S6). An additional factor explaining the divergence is the

315   pace of the regrowth curve. In contrast to the other models, MAgPIE assumes a single

316   response function per biome, irrespective of spatial differences in climate and soil conditions

317   within a biome, and thus ignores the effects of spatial differences within a biome, e.g. in terms

318   of annual precipitation or soil fertility on forest regrowth (Poorter *et al.*, 2016). Additionally,

319   MAgPIE does not account for disturbances. When looking at forest regrowth rates averaged

320   over different biomes it seems that tropical regrowth occurs much faster in MAgPIE than, for

321   example, in LPJ-GUESS (Fig. S7a).

322

323   Soil carbon

324   Compared to vegetation, modelled soil C changes in response to ADAFF activities are much

325   more diverse, with some DGVMs simulating net soil C losses upon afforestation (Figs. 1e,f,

326   2c). Soil C uptake in ADAFF is 62 GtC in IMAGE and 54 GtC in MAgPIE, which is

327   comparable to vegetation C uptake. In contrast, soil C changes in the DGVMs range between

328   -33 and +57 GtC. Soil C accumulation in LPJmL for the MAgPIE ADAFF scenario starts

329   significantly earlier than in the other models. As afforestation on pastures is common in

330   MAgPIE until around year 2070, this indicates a large soil C uptake potential in LPJmL for

331   pasture-forests transitions, which is also apparent in the LPJmL simulations driven by the

332   IMAGE ADAFF LU patterns. For BECCS, all models simulate small soil C losses (up to -16

333   GtC) which are generally larger in the LUMs than in the DGVMs. In both ADAFF and

334   BECCS, differences between LUMs and DGVMs in terms of soil C changes are more

335   pronounced for IMAGE-LU patterns than for MAgPIE-LU patterns.

336   The soil C emissions in JULES and ORCHIDEE for the ADAFF scenarios (and the relatively

337   low emissions for BECCS) might be partly caused by the simplistic representation of

338   agricultural management processes in these models. While LPJmL and LPJ-GUESS represent

339   croplands by specific crop PFTs and growing seasons, ORCHIDEE and JULES grow crops as

340   harvested grass (modified natural grass in ORCHIDEE, natural grass in JULES; see Table 1).

341   Additionally, ORCHIDEE does not include grazing of pastures, which means more biomass C

342   is transferred to the litter when the grass dies. Consequently, pastures and croplands have

343   larger soil C pools in ORCHIDEE and JULES, respectively, than if these processes were

344   accounted for, resulting in less soil C accumulation potential upon afforestation. To test

345   further how different representations of agriculture in the DGVMs affect soil C changes upon

346   afforestation we performed two sensitivity simulations with LPJ-GUESS in which we

347   simplified the representation of management processes following Pugh et al. (2015). In these

348   simulations, the rate of change in LPJ-GUESS soil C pools is reduced by 57% in the MAgPIE

349   ADAFF scenario (compared to the "standard" LPJ-GUESS simulations) when croplands are

350   represented by pastures (mimicking the representation of croplands in JULES), and by 49% in

351   the IMAGE ADAFF case when pastures are not harvested (mimicking the representation of

352   pastures in ORCHIDEE, not shown). Furthermore, LPJ-GUESS, JULES, and particularly

353   ORCHIDEE simulate a widespread decline in net primary productivity (NPP) upon

354   afforestation (Figs. 2f, S8) because in these models tropical grasslands (or croplands) are

355   often more productive than tropical forests. LPJmL, on the other hand, accounts for regional

356   yield gaps so cropland NPP is scaled down. Even though the fraction of NPP transferred to

357   the soil might differ across models (e.g. due to different mortality in secondary forests), this

358   suggests that the lower productivity of re-growing forests compared to agriculture also plays

359   an important role for the limited soil C accumulation (or emissions) in LPJ-GUESS, JULES,

360   and ORCHIDEE.

361

Cumulative CCS

CCS is calculated by multiplying the harvested C of bioenergy crops by a capture efficiency of 80% before geologic storage. A prescribed CCS trajectory was implemented in both LUMs, which means that annual global CCS rates are the same in IMAGE and MAgPIE. Cumulative CCS reaches 128 GtC in both LUMs by year 2099. In the DGVMs, cumulative CCS ranges from 37 to 130 GtC by year 2099 (Figs. 1g,h, 2d).

As the DGVMs used bioenergy production area from the LUMs and also the same assumptions about capture efficiency and storage capacity, the lower CCS calculated in most of the DGMVs has to arise mainly from differences in simulated bioenergy yields, including differences in the harvest index. Both LUMs assume rain-fed perennial and fast-growing second generation bioenergy crops (such as Miscanthus) to fulfil the CCS demand. LPJmL is the only DGVM representing dedicated bioenergy crops explicitly, but like the other DGVMs does not assume technological yield increases. This implies that the slightly larger cumulative CCS than in MAgPIE originates from higher initial yields. In contrast, LPJ-GUESS grows bioenergy as maize (with residues included for CCS), ORCHIDEE as crop grass, and JULES as natural grass (for harvest assumptions see Table S1). Consequently, average bioenergy yields are highest in LPJmL followed by LPJ-GUESS and then ORCHIDEE and JULES (Fig. S9). Cumulative CCS in all DGVMs apart from LPJmL is higher for IMAGE-LU patterns than for MAgPIE-LU patterns (Figs. 1g,h, 2d) because the larger cultivation area in IMAGE (Fig. S2c,d) outweighs lower average yields (Fig. S9). In the LUMs, the same trade-off between land expansion and yields results in equivalent global CCS rates in both LUMs.

383

Discussion

385   The C uptake potential of afforestation is largely restricted by historic C removal via

386   deforestation. Cumulative LUC emissions over the 1750-2015 period were ~190 GtC (Le

387   Quere et al., 2016), with a very large uncertainty arising from how different forms of land

388   management are considered in the simulations (Arneth et al., 2017) but also due to different

389   LUC hindcasts (Bayer et al., 2017). However, a possibly large fraction of agricultural area

390   will be needed for future food production (Boysen *et al.*, 2017a, Popp *et al.*, 2017) and CO_2

391   fertilizing effects on forest growth will likely be limited in RCP2.6. This suggests that

392   achieving 130 GtC net uptake via ADAFF might be challenging, consistent with results from

393   the DGVMs here (especially for MAgPIE-LU where avoided deforestation only plays a minor

394   role compared to afforestation). A limited (<150 GtC) C uptake potential via afforestation

395   within this century was also estimated in previous studies, despite very different methods and

396   assumptions (Lenton, 2010, and references therein). However, one recent study (Sonntag *et*

397   *al.*, 2016) found a much larger (215 GtC) uptake in a coupled Earth System Model (ESM) for

398   a high emission scenario (RCP8.5) when using RCP4.5 LU (afforestation, -700 Mha

399   agricultural land) instead of RCP8.5 LU (deforestation, +800 Mha agricultural land). The C

400   uptake was thus higher than in our study, but so were baseline deforestation rates, climate

401   impacts, and, particularly, differences in CO_2 fertilization (RCP8.5 *vs.* RCP2.6 in our study);

402   the high levels of CO_2 fertilization under RCP8.5 typically causes DGVMs to simulate much

403   larger C uptake in forests.

404   Some of the discrepancy in total C uptake between the LUMs and the DGVMs in the ADAFF

405   scenarios originates from differences in vegetation C uptake, especially for MAgPIE. Natural

406   forest regrowth upon agricultural abandonment is implemented in all DGVMs and IMAGE,

407   while MAgPIE assumes managed regrowth according to prescribed, region-specific growth

408   curves towards the biomass density of potential natural vegetation (Humpenöder *et al.*, 2014).

409   Observational studies differ substantially in reported forest regrowth rates (Krause *et al.*,

410 2016, and references therein). Biomass accumulation in tropical forests has often been

411 reported to slow down a few decades after agricultural cessation, with aboveground biomass

412 levels (representing ~80% of total biomass, Cairns *et al.*, 1997) of mature tropical forests

413 being reached within ca. 66-90 years (Anderson-Teixeira *et al.*, 2016, Poorter *et al.*, 2016),

414 and belowground biomass needing more time to recover, especially following shifting

415 agriculture (Martin *et al.*, 2013). Poorter et al. (2016) also found slower accumulation rates in

416 dry (<1500 mm) compared to wet (>2500 mm) environments. In comparison, tropical (22°S-

417 20°N as in Poorter et al.) afforestation in the MAgPIE ADAFF scenario occurs in relatively

418 dry regions, with an average precipitation of 1682 mm yr^{-1}. While we can only quantify

419 tropical recovery times (90% of old forest biomass) for MAgPIE (47 years; Fig. S7a) and

420 LPJ-GUESS (~150 years in tropical Africa), the vegetation C uptake is similar across all

421 DGVMs. The observational studies point towards typical recovery times that lie in the middle

422 of this range. This suggests that, assuming that afforestation will mostly occur as natural

423 regrowth, tropical biomass accumulation rates might be overestimated in MAgPIE. The LPJ-

424 GUESS recovery times of Krause et al. (2016) are, however, not directly comparable to these

425 observations, as the LPJ-GUESS simulations allowed natural stand-replacing disturbances

426 (e.g. fire, wind-throw) to occur in these recovering forests, slowing the recovery rate, whilst

427 this is not likely to be the case in the chronosequence observations, which typically age the

428 stand from last disturbance. Evaluation of forest regrowth rates in DGVMs, particularly in

429 tropical forests, will be important to constrain uncertainty in ADAFF potential.

430 Degraded forests also represent an uncertainty in our IMAGE scenarios. JULES represented

431 degraded forests as natural vegetation, whereas the other DGVMs, simply for consistency,

432 followed the IMAGE assumption of degraded forests being grassland. In reality, degraded

433 forests likely represents a mixture between both approaches, with aboveground biomass on

434 average being 70% lower than in undisturbed forests (Asner et al., 2010). Clearly, assuming a

435 degraded forest being a grassland will overestimate vegetation C uptake potential when

436 degraded forests are converted back to forests (in IMAGE ~50% of the avoided deforestation

437 and afforestation area by end-century is from degraded forests; see Table S2). Additionally,

438 the mismatch between forest loss and agricultural gain reported by FAO (based on which the

439 degraded forest class was introduced in IMAGE) might be largely explained by shifting

440 cultivation (Houghton and Nassikas, 2017). However, most LUMs/DGVMs so far cannot

441 adequately simulate shifting cultivation due to not explicitly representing forest demography.

442 The representation of forest degradation thus remains a challenge for LUMs and DGVMs.

443 Soil C changes contribute most to variations in total C uptake across models. Differences in

444 simulated present-day soil C stocks are hardly surprising as global soil C estimates are very

445 uncertain (Scharlemann *et al.*, 2014) and large variations across DGVMs and ESMs have

446 been reported before (Anav *et al.*, 2013, Tian *et al.*, 2015, Todd-Brown *et al.*, 2013).

447 Numerous studies explored soil C changes following LUC (Smith *et al.*, 2016b, and

448 references therein), but there is still substantial disagreement in terms of the magnitude of

449 change for most land-cover transitions. While studies agree that transitions from forests to

450 croplands reduce soil C (and vice versa), patterns are more diverse for conversions to/from

451 grassland, depending on management intensity, climate, and soils (McSherry and Ritchie,

452 2013, Powers *et al.*, 2011). The picture is further complicated by evidence that the existing

453 field observations in the tropics might not be representative for many tropical landscapes

454 (Powers *et al.*, 2011).

455 The LUC scenarios from the LUMs differ in terms of converted land-cover types: in

456 MAgPIE, afforestation partly takes place on former croplands (especially before year 2025

457 and after 2070). MAgPIE assumes initial litter C (both in croplands and pastures) to be

458 completely depleted and, based on IPCC guidelines, to be replenished within 20 years

459 following agricultural abandonment. Soil C in former croplands is assumed to increase from

460   the grid-cell specific average soil C density of cropland and natural vegetation towards the

461   soil C density of natural vegetation within 20 years (Humpenöder *et al.*, 2014). However, a

462   litter C density of zero and an assumed time frame of 20 years until soil C reaches equilibrium

463   appear questionable. In fact, some studies report soil C to decrease during the first years after

464   cropland cessation (Deng *et al.*, 2016), and subsequent C accumulation is usually slow and

465   proceeds over several decades or even centuries (Silver *et al.*, 2000). In contrast to the

466   prescribed recovery implemented in MAgPIE, IMAGE simulates soil C changes dynamically

467   within LPJmL. However, the contribution of soils to total C uptake is comparable to MAgPIE

468   even though ADAFF activities in IMAGE are largely restricted to pasture-forest transitions.

469   In reality, afforestation on grasslands (or avoided conversion from forests to grasslands) has

470   even less soil C uptake potential than on croplands; soil C depletions in pastures/grasslands

471   relative to forests are generally low (Don *et al.*, 2011, Laganiere *et al.*, 2010) and in many

472   cases grasslands even store more soil C than the replacing forests (Li et al., submitted; Guo

473   and Gifford, 2002, Poeplau *et al.*, 2011, Powers *et al.*, 2011). Additionally, declines in soil C

474   have been reported during the first years of forest regrowth before accumulation occurs and

475   net accumulation is often only achieved after several decades (Paul *et al.*, 2002, Poeplau *et*

476   *al.*, 2011). Consequently, the rapid soil C uptake in the LUMs for ADAFF is likely

477   overoptimistic, while limited soil C accumulation (compared to vegetation C) in response to

478   afforestation as simulated by some DGVMs seems to be more realistic. However, historic

479   agriculture has likely resulted in substantial net soil C emissions (Sanderman *et al.*, 2017,

480   Smith *et al.*, 2016b), so large soil C losses in response to afforestation as simulated by

481   ORCHIDEE are also unlikely, especially for the MAgPIE ADAFF scenario (where croplands

482   are preferentially afforested).

483   One likely reason for the large discrepancy in simulated soil C changes in response to

484   afforestation is the simulated change in ecosystem productivity. Todd-Brown et al. (2013)

485   showed that soil C stocks in ESMs are closely coupled to simulated NPP. In our simulations,

486   simulated changes in NPP in response to ADAFF activities are very different across models,

487   which partly explains differences in soil C accumulation. Modelling work by DeFries (2002)

488   suggests that regional impacts of LUC on NPP are highly variable, depending on management

489   intensity and original vegetation cover, and that cropland productivity is higher compared to

490   forests in temperate regions. The relatively high productivity of temperate crops seems to be

491   confirmed for European studies (Ciais *et al.*, 2010, Luyssaert *et al.*, 2010), but estimates are

492   highly dependent on the data source from which NPP is derived. In the tropics, observations

493   suggest crop productivity at many locations to be lower than for forests (Cleveland *et al.*,

494   2015, Monfreda *et al.*, 2008). As afforestation in our scenarios is mostly concentrated in the

495   tropics, the NPP decrease following afforestation in most DGVMs seems to be unrealistic.

496   A second potentially important reason for the large differences in simulated soil C uptake is

497   different amounts of C removed from agricultural land. Soil C recovery following agricultural

498   cessation has recently been simulated with a different version of LPJ-GUESS (croplands were

499   represented by tilled, fertilized, and harvested grassland rather than specific crop PFTs) and

500   showed reasonable agreement with observations (Krause *et al.*, 2016). ORCHIDEE and

501   JULES represent fewer management processes and therefore may underestimate soil C uptake

502   potential in ADAFF (but also losses in BECCS); the incorporation of harvest (not included in

503   ORCHIDEE pastures) and the representation of crops by specific crop PFTs (including

504   tillage), instead of grasses, substantially increases soil C depletions on agricultural land in

505   LPJ-GUESS (Pugh *et al.*, 2015). However, there are also observations suggesting that

506   moderately intensive grazing might actually increase soil C stocks in C4-dominated

507   grasslands (McSherry and Ritchie, 2013, Navarrete *et al.*, 2016), a process the DGVMs likely

508   do not capture well.

509   The LUMs did not include deforestation emissions ("carbon debt", Fargione *et al.*, 2008) in

510   their BECCS CDR target. This is a common procedure in BECCS scenarios (or at least LUC

511   emissions are often not seperated from fossil fuel emissions, e.g. Smith *et al.*, 2016a). For two

512   bioenergy scenarios (600 and 800 Mha production area made available via either

513   deforestation or agricultural abandonment, RCP2.6 climate) comparable in terms of area and

514   climate changes to our scenarios, a modelling study by Wiltshire and Davies-Barnard (2015)

515   estimated vegetation C losses of 70 and 0 GtC and, using average depletions from Guo and

516   Gillford (2002), soil C losses of 20 and 60 GtC. In our simulations, vegetation and soil C

517   emissions are relatively small, but our study still confirms that these emissions should not be

518   neglected when considering bioenergy as an option to achieve negative emissions.

519   Cumulative CCS in BECCS differs substantially across models, ranging between 37 GtC and

520   130 GtC in the DGVMs, and reaching 128 GtC in both LUMs. By comparison, Wiltshire and

521   Davies-Barnard (2015) found 75 and 200 GtC for the two comparable scenarios, which is

522   similar to the 100-230 GtC range reported by Smith et al. (2016a) for IAM scenarios

523   consistent with the 2°C target. Recently, Boysen et al. (2017a) estimated land availability for

524   bioenergy production in LPJmL. They found that in the best case scenario, biomass

525   plantations on abandoned agricultural land could deliver up to 350 GtC by 2100 (but likely

526   much less), and potentially more if plantations would replace natural ecosystems. In our

527   study, bioenergy area was prescribed by the LUMs and differences in CCS across models

528   originate from simulated bioenergy crop yields. The LUMs and LPJmL represent these crops

529   as dedicated bioenergy crops, mimicking characteristics of perennial energy crops like

530   switchgrass or Miscanthus. Bioenergy yields in LPJmL have recently been evaluated against

531   observations and showed reasonable results but were hindered by limited experimental data in

532   the tropics (Heck *et al.*, 2016). The other DGVMs grow bioenergy crops as maize (LPJ-

533   GUESS), productive grass (ORCHIDEE), or natural grass (JULES). JULES and ORCHIDEE

534   also do not increase the harvest index for bioenergy crops relative to food crops. Additionally,

535   the LUMs assume technological yield increases over time, resulting in higher average yields

536   than in most DGVMs. While research of dedicated bioenergy crops is just in its infancy and

537   thus on the one hand promises high potential, there is also evidence that yield increases

538   observed over the last decades for cereals have recently slowed down (Alexandratos and

539   Bruinsma, 2012). In fact, much of the historic yield increase was achieved via increasing the

540   harvest index and fertilizer application, processes that are unlikely to substantially affect

541   bioenergy yields (Searle and Malins, 2014). It also remains to be seen what bioenergy yield

542   will be attainable in more marginal lands compared to sites where these crops are typically

543   grown today (Searle and Malins, 2014). Consequently, what bioenergy yields we can expect

544   in the future is controversial, with the optimistic assumptions made in IAMs/LUMs being

545   plausible, but towards the upper bound of uncertainty (Creutzig, 2016).

546   We conclude that forest maintenance and expansion, as well as large-scale bioenergy

547   production combined with CCS, offer the potential to remove substantial amounts of C from

548   the atmosphere and thus can help to mitigate climate change. However, the size of the

549   removal is highly uncertain, and may be much less than previously assumed in IAM/LUM

550   scenarios consistent with the 2°C target (Boysen *et al.*, 2017b, Rogelj *et al.*, 2015, Smith *et*

551   *al.*, 2016a, Tavoni and Socolow, 2013, Wiltshire and Davies-Barnard, 2015); the C uptake

552   simulated by the LUMs is only achieved in one out of 16 combinations of mitigation LUC

553   scenarios and DGVMs. The main reasons for the typically lower C uptake in the DGVMs as

554   initially implemented in the LUMs are slower soil C accumulation (or even losses) following

555   afforestation, different assumptions on potential vegetation C stocks, lower growth rates of

556   forests, and lower bioenergy yields. Clearly the per-area C uptake (and thus the land demand)

557   in land-based mitigation scenarios depends on assumptions made about vegetation and soil

558   processes in the IAMs/LUMs. An improved implementation of land-based CDR options in

559   both kinds of models, LUMs and DGVMs, as well as a deeper interaction between both is

560   necessary to draw more robust conclusions about the potential contribution of land

561   management to climate stabilization. While the LUMs should emphasize the large uncertainty

562   in assumed yields from bioenergy plantations, the DGVMs need to improve the

563   parameterizations of managed herbaceous vegetation, particularly bioenergy crops (and also

564   woody bioenergy), as well as regrowth of managed forests for afforestation. Field

565   observations should focus on studying bioenergy crop productivity under commercial

566   production conditions. Additionally, the LUMs and some DGVMs need to reconsider their

567   assumptions about soil C sequestration rates following afforestation. More detailed

568   information about grazing intensities on grasslands, and a clear differentiation between

569   natural grasslands and intensively managed pastures in observational studies might also help

570   to reduce the uncertainty in soil C changes following LUC (Navarrete *et al.*, 2016).

571   In this study we only address the uncertainty in land-based mitigation arising from potential C

572   uptake for a prescribed available area. However, the establishment of negative emissions from

573   land management could also be hindered by unacceptable social or ecological side-effects

574   (Kartha and Dooley, 2016, Krause *et al.*, 2017, Smith *et al.*, 2016a), biophysical and

575   biogeochemical climate impacts beyond C (Boysen *et al.*, 2017a, Krause *et al.*, 2017, Smith *et*

576   *al.*, 2016a), irreversible effects of overshooting CO_2 concentrations (Kartha and Dooley,

577   2016, Tokarska and Zickfeld, 2015), or simply because CCS turns out to be technologically

578   infeasible at commercial scale. There is also strong evidence that the timescales for shifts in

579   farming systems to be realized may be of the order of several decades, substantially delaying

580   the onset of negative emissions from BECCS (Alexander *et al.*, 2013; Brown et al.,

581   submitted). Combining these unknowns and caveats with the large uncertainty in uptake

582   potential identified in this study suggests that relying on negative emissions to mitigate

583   climate change is a very high-risk strategy.

584

Acknowledgements

594

Conflict of Interest

596 The authors declare no conflict of interest.

597

References

599 Alexander P, Moran D, Rounsevell MDA, Smith P (2013) Modelling the perennial energy crop market:
600 the role of spatial diffusion. *Journal of the Royal Society Interface,* **10**,
601 doi:10.1098/Rsif.2013.0656.

602 Alexandratos N, Bruinsma J (2012) World agriculture towards 2030/2050: the 2012 revision. Rome,
603 FAO.

604 Anav A, Friedlingstein P, Kidston M *et al.* (2013) Evaluating the Land and Ocean Components of the
605 Global Carbon Cycle in the CMIP5 Earth System Models. *Journal of Climate,* **26**, 6801-6843,
606 doi:10.1175/Jcli-D-12-00417.1.

607 Anderson-Teixeira KJ, Wang MMH, Mcgarvey JC, Lebauer DS (2016) Carbon dynamics of mature and
608 regrowth tropical forests derived from a pantropical database (TropForC-db). *Global Change*
609 *Biology,* **22**, 1690-1709, doi:10.1111/gcb.13226.

610 Anderson K, Peters G (2016) The trouble with negative emissions. *Science,* **354**, 182-183,
611   doi:10.1126/science.aah4567.

612 Arneth A, Sitch S, Pongratz J *et al.* (2017) Historical carbon dioxide emissions caused by land-use
613   changes are possibly larger than assumed. *Nature Geoscience,* **10**, 79-84,
614   doi:10.1038/NGEO2882.

615 Asner GP, Powell GVN, Mascaro J *et al.* (2010) High-resolution forest carbon stocks and emissions in
616   the Amazon. *Proceedings of the National Academy of Sciences of the United States of*
617   *America,* **107**, 16738-16742, doi:10.1073/pnas.1004875107.

618 Bayer AD, Lindeskog M, Pugh TaM, Anthoni PM, Fuchs R, Arneth A (2017) Uncertainties in the land-
619   use flux resulting from land-use change reconstructions and gross land transitions. *Earth*
620   *System Dynamics,* **8**, 91-111, doi:10.5194/esd-8-91-2017.

621 Best MJ, Pryor M, Clark DB *et al.* (2011) The Joint UK Land Environment Simulator (JULES), model
622   description - Part 1: Energy and water fluxes. *Geoscientific Model Development,* **4**, 677-699,
623   doi:10.5194/gmd-4-677-2011.

624 Bondeau A, Smith PC, Zaehle S *et al.* (2007) Modelling the role of agriculture for the 20th century
625   global terrestrial carbon balance. *Global Change Biology,* **13**, 679-706, doi:10.1111/j.1365-
626   2486.2006.01305.x.

627 Boysen LR, Lucht W, Gerten D (2017a) Trade-offs for food production, nature conservation and
628   climate limit the terrestrial carbon dioxide removal potential. *Global Change Biology*,
629   doi:10.1111/gcb.13745.

630 Boysen LR, Lucht W, Gerten D, Heck V, Lenton TM, Schellnhuber HJ (2017b) The limits to global-
631   warming mitigation by terrestrial carbon removal. *Earths Future,* **5**, 463-474,
632   doi:10.1002/2016EF000469.

633 Cairns MA, Brown S, Helmer EH, Baumgardner GA (1997) Root biomass allocation in the world's
634   upland forests. *Oecologia,* **111**, 1-11, doi:10.1007/s004420050201.

635 Ciais P, Wattenbach M, Vuichard N *et al.* (2010) The European carbon balance. Part 2: croplands.
636   *Global Change Biology,* **16**, 1409-1428, doi:10.1111/j.1365-2486.2009.02055.x.

637 Clark DB, Mercado LM, Sitch S *et al.* (2011) The Joint UK Land Environment Simulator (JULES), model
638   description - Part 2: Carbon fluxes and vegetation dynamics. *Geoscientific Model*
639   *Development,* **4**, 701-722, doi:10.5194/gmd-4-701-2011.

640 Cleveland CC, Taylor P, Chadwick KD *et al.* (2015) A comparison of plot-based satellite and Earth
641   system model estimates of tropical forest net primary production. *Global Biogeochemical*
642   *Cycles,* **29**, 626-644, doi:10.1002/2014GB005022.

643 Creutzig F (2016) Economic and ecological views on climate change mitigation with bioenergy and
644   negative emissions. *Global Change Biology Bioenergy,* **8**, 4-10, doi:10.1111/gcbb.12235.

645 Defries R (2002) Past and future sensitivity of primary production to human modification of the
646   landscape. *Geophysical Research Letters,* **29**, doi:10.1029/2001gl013620.

647 Deng L, Zhu G, Tang Z, Shangguan Z (2016) Global patterns of the effects of land-use changes on soil
648   carbon stocks. *Global Ecology and Conservation,* **5**, 127-138,
649   doi:10.1016/j.gecco.2015.12.004.

650 Doelman JC, Stehfest E, Tabeau A *et al.* (2018) Exploring SSP land-use dynamics using the IMAGE
651   model: Regional and gridded scenarios of land-use change and land-based climate change
652   mitigation. *Global Environmental Change,* **48**, 119-135, doi:10.1016/j.gloenvcha.2017.11.014.

653 Don A, Schumacher J, Freibauer A (2011) Impact of tropical land-use change on soil organic carbon
654   stocks - a meta-analysis. *Global Change Biology,* **17**, 1658-1670, doi:10.1111/j.1365-
655   2486.2010.02336.x.

656 Fargione J, Hill J, Tilman D, Polasky S, Hawthorne P (2008) Land clearing and the biofuel carbon debt.
657   *Science,* **319**, 1235-1238, doi:10.1126/science.1152747.

658 Fuss S, Canadell JG, Peters GP *et al.* (2014) COMMENTARY: Betting on negative emissions. *Nature*
659   *Climate Change,* **4**, 850-853, doi:10.1038/nclimate2392.

660 Gasser T, Guivarch C, Tachiiri K, Jones CD, Ciais P (2015) Negative emissions physically needed to
661   keep global warming below 2 degrees C. *Nature Communications,* **6**,
662   doi:10.1038/Ncomms8958.

663 Guo LB, Gifford RM (2002) Soil carbon stocks and land use change: a meta analysis. *Global Change*
664   *Biology,* **8**, 345-360, doi:10.1046/j.1354-1013.2002.00486.x.

665 Heck V, Gerten D, Lucht W, Boysen LR (2016) Is extensive terrestrial carbon dioxide removal a 'green'
666   form of geoengineering? A global modelling study. *Global and Planetary Change,* **137**, 123-
667   130, doi:10.1016/j.gloplacha.2015.12.008.

668 Hempel S, Frieler K, Warszawski L, Schewe J, Piontek F (2013) A trend-preserving bias correction - the
669   ISI-MIP approach. *Earth System Dynamics,* **4**, 219-236, doi:10.5194/esd-4-219-2013.

670 Houghton RA, Nassikas AA (2017) Negative emissions from stopping deforestation and forest
671   degradation, globally. *Global Change Biology*, 1-10, doi:10.1111/gcb.13876.

672 Humpenöder F, Popp A, Dietrich JP *et al.* (2014) Investigating afforestation and bioenergy CCS as
673   climate change mitigation strategies. *Environmental Research Letters,* **9**, doi:10.1088/1748-
674   9326/9/6/064029.

675 Johnson MO, Galbraith D, Gloor M *et al.* (2016) Variation in stem mortality rates determines patterns
676   of above-ground biomass in Amazonian forests: implications for dynamic global vegetation
677   models. *Global Change Biology,* **22**, 3996-4013, doi:10.1111/gcb.13315.

678 Kartha S, Dooley K (2016) The risks of relying on tomorrow's 'negative emissions' to guide today's
679   mitigation action. Stockholm Environment Institute.

680 Klein D, Luderer G, Kriegler E *et al.* (2014) The value of bioenergy in low stabilization scenarios: an
681   assessment using REMIND-MAgPIE. *Climatic Change,* **123**, 705-718, doi:10.1007/s10584-013-
682   0940-z.

683 Klein Goldewijk K, Beusen A, Van Drecht G, De Vos M (2011) The HYDE 3.1 spatially explicit database
684   of human-induced global land-use change over the past 12,000 years. *Global Ecology and*
685   *Biogeography,* **20**, 73-86, doi:10.1111/j.1466-8238.2010.00587.x.

686 Krause A, Pugh TaM, Bayer AD *et al.* (2017) Global consequences of afforestation and bioenergy
687   cultivation on ecosystem service indicators. *Biogeosciences,* **14**, 4829–4850, doi:10.5194/bg-
688   14-4829-2017.

689 Krause A, Pugh TaM, Bayer AD, Lindeskog M, Arneth A (2016) Impacts of land-use history on the
690   recovery of ecosystems after agricultural abandonment. *Earth System Dynamics,* **7**, 745-766,
691   doi:10.5194/esd-7-745-2016.

692 Krinner G, Viovy N, De Noblet-Ducoudre N *et al.* (2005) A dynamic global vegetation model for
693   studies of the coupled atmosphere-biosphere system. *Global Biogeochemical Cycles,* **19**,
694   doi:10.1029/2003gb002199.

695 Laganiere J, Angers DA, Pare D (2010) Carbon accumulation in agricultural soils after afforestation: a
696   meta-analysis. *Global Change Biology,* **16**, 439-453, doi:10.1111/j.1365-2486.2009.01930.x.

697 Le Quere C, Andrew RM, Canadell JG *et al.* (2016) Global Carbon Budget 2016. *Earth System Science*
698   *Data,* **8**, 605-649, doi:10.5194/essd-8-605-2016.

699 Lenton TM (2010) The potential for land-based biological CO_2 removal to lower future atmospheric
700   CO_2 concentration. *Carbon Management,* **1**, 145-160, doi:10.4155/Cmt.10.12.

701 Lenton TM, Vaughan NE (2009) The radiative forcing potential of different climate geoengineering
702   options. *Atmospheric Chemistry and Physics,* **9**, 5539-5561, doi:10.5194/acp-9-5539-2009.

703 Lotze-Campen H, Muller C, Bondeau A, Rost S, Popp A, Lucht W (2008) Global food demand,
704   productivity growth, and the scarcity of land and water resources: a spatially explicit
705   mathematical programming approach. *Agricultural Economics,* **39**, 325-338,
706   doi:10.1111/j.1574-0862.2008.00336.x.

707 Luyssaert S, Ciais P, Piao SL *et al.* (2010) The European carbon balance. Part 3: forests. *Global Change*
708   *Biology,* **16**, 1429-1450, doi:10.1111/j.1365-2486.2009.02056.x.

709 Martin PA, Newton AC, Bullock JM (2013) Carbon pools recover more quickly than plant biodiversity
710   in tropical secondary forests. *Proceedings of the Royal Society B-Biological Sciences,* **280**,
711   doi:10.1098/Rspb.2013.2236.

712 Mcsherry ME, Ritchie ME (2013) Effects of grazing on grassland soil carbon: a global review. *Global*
713   *Change Biology,* **19**, 1347-1357, doi:10.1111/gcb.12144.

714 Meinshausen M, Smith SJ, Calvin K *et al.* (2011) The RCP greenhouse gas concentrations and their
715   extensions from 1765 to 2300. *Climatic Change,* **109**, 213-241, doi:10.1007/s10584-011-
716   0156-z.

717 Monfreda C, Ramankutty N, Foley JA (2008) Farming the planet: 2. Geographic distribution of crop
718   areas, yields, physiological types, and net primary production in the year 2000. *Global*
719   *Biogeochemical Cycles,* **22**, doi:10.1029/2007gb002947.

720 Navarrete D, Sitch S, Aragao LEOC, Pedroni L (2016) Conversion from forests to pastures in the
721 Colombian Amazon leads to contrasting soil carbon dynamics depending on land
722 management practices. *Global Change Biology,* **22**, 3503-3517, doi:10.1111/gcb.13266.

723 Olin S, Lindeskog M, Pugh TaM *et al.* (2015) Soil carbon management in large-scale Earth system
724 modelling: implications for crop yields and nitrogen leaching. *Earth System Dynamics,* **6**, 745-
725 768, doi:10.5194/esd-6-745-2015.

726 Paul KI, Polglase PJ, Nyakuengama JG, Khanna PK (2002) Change in soil carbon following
727 afforestation. *Forest Ecology and Management,* **168**, 241-257, doi:10.1016/S0378-
728 1127(01)00740-X.

729 Poeplau C, Don A, Vesterdal L, Leifeld J, Van Wesemael B, Schumacher J, Gensior A (2011) Temporal
730 dynamics of soil organic carbon after land-use change in the temperate zone - carbon
731 response functions as a model approach. *Global Change Biology,* **17**, 2415-2427,
732 doi:10.1111/j.1365-2486.2011.02408.x.

733 Poorter L, Ongers FB, Aide TM *et al.* (2016) Biomass resilience of Neotropical secondary forests.
734 *Nature,* **530**, 211-214, doi:10.1038/nature16512.

735 Popp A, Calvin K, Fujimori S *et al.* (2017) Land-use futures in the shared socio-economic pathways.
736 *Global Environmental Change-Human and Policy Dimensions,* **42**, 331-345,
737 doi:10.1016/j.gloenvcha.2016.10.002.

738 Popp A, Humpenoder F, Weindl I *et al.* (2014a) Land-use protection for climate change mitigation.
739 *Nature Climate Change,* **4**, 1095-1098, doi:10.1038/Nclimate2444.

740 Popp A, Rose SK, Calvin K *et al.* (2014b) Land-use transition for bioenergy and climate stabilization:
741 model comparison of drivers, impacts and interactions with other land use based mitigation
742 options. *Climatic Change,* **123**, 495-509, doi:10.1007/s10584-013-0926-x.

743 Powers JS, Corre MD, Twine TE, Veldkamp E (2011) Geographic bias of field observations of soil
744 carbon stocks with tropical land-use changes precludes spatial extrapolation. *Proceedings of*
745 *the National Academy of Sciences of the United States of America,* **108**, 6318-6322,
746 doi:10.1073/pnas.1016774108.

747 Pugh TaM, Arneth A, Olin S *et al.* (2015) Simulated carbon emissions from land use change are
748 substantially enhanced by accounting for agricultural management. *Environmental Research*
749 *Letters,* **10**, doi:10.1088/1748-9326/10/12/124008.

750 Riahi K, Van Vuuren DP, Kriegler E *et al.* (2017) The Shared Socioeconomic Pathways and their
751 energy, land use, and greenhouse gas emissions implications: An overview. *Global*
752 *Environmental Change-Human and Policy Dimensions,* **42**, 153-168,
753 doi:10.1016/j.gloenvcha.2016.05.009.

754 Rogelj J, Luderer G, Pietzcker RC, Kriegler E, Schaeffer M, Krey V, Riahi K (2015) Energy system
755 transformations for limiting end-of-century warming to below 1.5 degrees C. *Nature Climate*
756 *Change,* **5**, 519–527, doi:10.1038/nclimate2572.

757 Sanderman J, Hengl T, Fiske GJ (2017) Soil carbon debt of 12,000 years of human land use.
758   *Proceedings of the National Academy of Sciences of the United States of America,* **114**, 9575-
759   9580, doi:10.1073/pnas.1706103114.

760 Sanderson BM, O'neill BC, Tebaldi C (2016) What would it take to achieve the Paris temperature
761   targets? *Geophysical Research Letters,* **43**, 7133-7142, doi:10.1002/2016GL069563.

762 Scharlemann JPW, Tanner EVJ, Hiederer R, Kapos V (2014) Global soil carbon: understanding and
763   managing the largest terrestrial carbon pool. *Carbon Management,* **5**, 81-91,
764   doi:10.4155/Cmt.13.77.

765 Searle SY, Malins CJ (2014) Will energy crop yields meet expectations? *Biomass & Bioenergy,* **65**, 3-
766   12, doi:10.1016/j.biombioe.2014.01.001.

767 Silver WL, Ostertag R, Lugo AE (2000) The potential for carbon sequestration through reforestation of
768   abandoned tropical agricultural and pasture lands. *Restoration Ecology,* **8**, 394-407,
769   doi:10.1046/j.1526-100x.2000.80054.x.

770 Sitch S, Smith B, Prentice IC *et al.* (2003) Evaluation of ecosystem dynamics, plant geography and
771   terrestrial carbon cycling in the LPJ dynamic global vegetation model. *Global Change Biology,*
772   **9**, 161-185, doi:10.1046/j.1365-2486.2003.00569.x.

773 Smith B, Warlind D, Arneth A, Hickler T, Leadley P, Siltberg J, Zaehle S (2014) Implications of
774   incorporating N cycling and N limitations on primary production in an individual-based
775   dynamic vegetation model. *Biogeosciences,* **11**, 2027-2054, doi:10.5194/bg-11-2027-2014.

776 Smith P, Davis SJ, Creutzig F *et al.* (2016a) Biophysical and economic limits to negative CO2 emissions.
777   *Nature Climate Change,* **6**, 42-50, doi:10.1038/Nclimate2870.

778 Smith P, House JI, Bustamante M *et al.* (2016b) Global change pressures on soils from land use and
779   management. *Global Change Biology,* **22**, 1008-1028, doi:10.1111/gcb.13068.

780 Sonntag S, Pongratz J, Reick CH, Schmidt H (2016) Reforestation in a high-CO2 world-Higher
781   mitigation potential than expected, lower adaptation potential than hoped for. *Geophysical*
782   *Research Letters,* **43**, 6546-6553, doi:10.1002/2016GL068824.

783 Stehfest E, Van Vuuren D, Kram T *et al.* (2014) Integrated Assessment of Global Environmental
784   Change with IMAGE 3.0 : Model description and policy applications. The Hague: PBL
785   Netherlands Environmental Assessment Agency.

786 Tavoni M, Socolow R (2013) Modeling meets science and technology: an introduction to a special
787   issue on negative emissions. *Climatic Change,* **118**, 1-14, doi:10.1007/s10584-013-0757-9.

788 Tian HQ, Lu CQ, Yang J *et al.* (2015) Global patterns and controls of soil organic carbon dynamics as
789   simulated by multiple terrestrial biosphere models: Current status and future directions.
790   *Global Biogeochemical Cycles,* **29**, 775-792, doi:10.1002/2014GB005021.

791 Todd-Brown KEO, Randerson JT, Post WM, Hoffman FM, Tarnocai C, Schuur EaG, Allison SD (2013)
792   Causes of variation in soil carbon simulations from CMIP5 Earth system models and
793   comparison with observations. *Biogeosciences,* **10**, 1717-1736, doi:10.5194/bg-10-1717-
794   2013.

795   Tokarska KB, Zickfeld K (2015) The effectiveness of net negative carbon dioxide emissions in reversing
796   anthropogenic climate change. *Environmental Research Letters,* **10**, doi:10.1088/1748-
797   9326/10/9/094013.

798   Williamson P (2016) Scrutinize CO2 removal methods. *Nature,* **530**, 153-155, doi:10.1038/530153a.

799   Wiltshire A, Davies-Barnard T (2015) Planetary limits to BECCS negative emissions. In: *AVOID 2*
800   *WPD.2a Report 1.*

801

802

803

804

805

806

807

808

809

810

811

812

813

814

Tables

Table 1: Overview of major DGVM differences relevant to this study. A more detailed

version of the table can be found in the supplement (Table S1).

Variable or process	DGVM			
	LPJ-GUESS	ORCHIDEE	JULES	LPJmL
Spatial resolution	0.5º x 0.5º	2° x 2°	0.5° x 0.5°	
Nitrogen cycle	yes	no		
Implementation of LU patterns from the LUMs into the DGVM	absolute cropland, pasture, and natural area prescribed by LUMs, PFT distribution on natural land is simulated dynamically	changes in cropland, pasture, and forest vs. other natural area prescribed by LUMs, forest area and PFT distribution (static on natural land) in year 2005 according to internal map (from European Space Agency)	absolute cropland, pasture, and natural area prescribed by LUMs, PFT distribution on natural land is simulated dynamically	
Implementation of agricultural expansion	all natural PFTs are reduced proportionally		grasslands are reduced first, then shrubs, then forests	all natural PFTs are reduced proportionally
Representation of degraded forests (for IMAGE-LU patterns only)	as pasture	as natural grassland	as natural vegetation (forests or natural grassland)	as pasture
Forest (re)growth dynamics	cohort approach (competition between different age classes), natural regrowth	dilution approach (one average individual per PFT), natural regrowth		
Pasture management	harvest, woody vegetation is prevented from growing	no harvest, woody vegetation is prevented from growing	harvest*, woody vegetation is prevented from growing	harvest with variable intensity, woody vegetation is prevented from

				growing
Cropland management	four crop PFTs (temperate wheat, maize, rice, temperate other), variable sowing and harvest date, tillage, irrigation, fertilization, dynamic potential heat unit calculation, woody vegetation is prevented from growing	C3 + C4 crop grass (similar phenology as natural grass but adapted maximum LAI and slightly modified critical temperature and humidity parameters), harvest, woody vegetation is prevented from growing	C3 + C4 grass, harvest, woody vegetation is prevented from growing	12 crop PFTs, variable sowing and harvest date, irrigation, woody vegetation is prevented from growing
Dedicated bioenergy crop PFTs	no (grown as maize)	no (grown as C3 or C4 crop grass)	no (grown as C3 or C4 grass)	yes (fast-growing C4 grass, temperate and tropical short rotation coppices)

818   *Pastures were treated as cropland in these JULES simulations. Normally pastures are not

819   harvested in JULES.

820

821

822

823

824

825

826

Figure captions

IMAGE-LU   **MAgPIE-LU**

(a) total carbon (including CCS in BECCS)   (b) total carbon (including CCS in BECCS)

(c) vegetation carbon   (d) vegetation carbon

(e) litter and soil carbon   (f) litter and soil carbon

(g) cumulative CCS   (h) cumulative CCS

IMAGE/MAgPIE   JULES   ADAFF scenarios
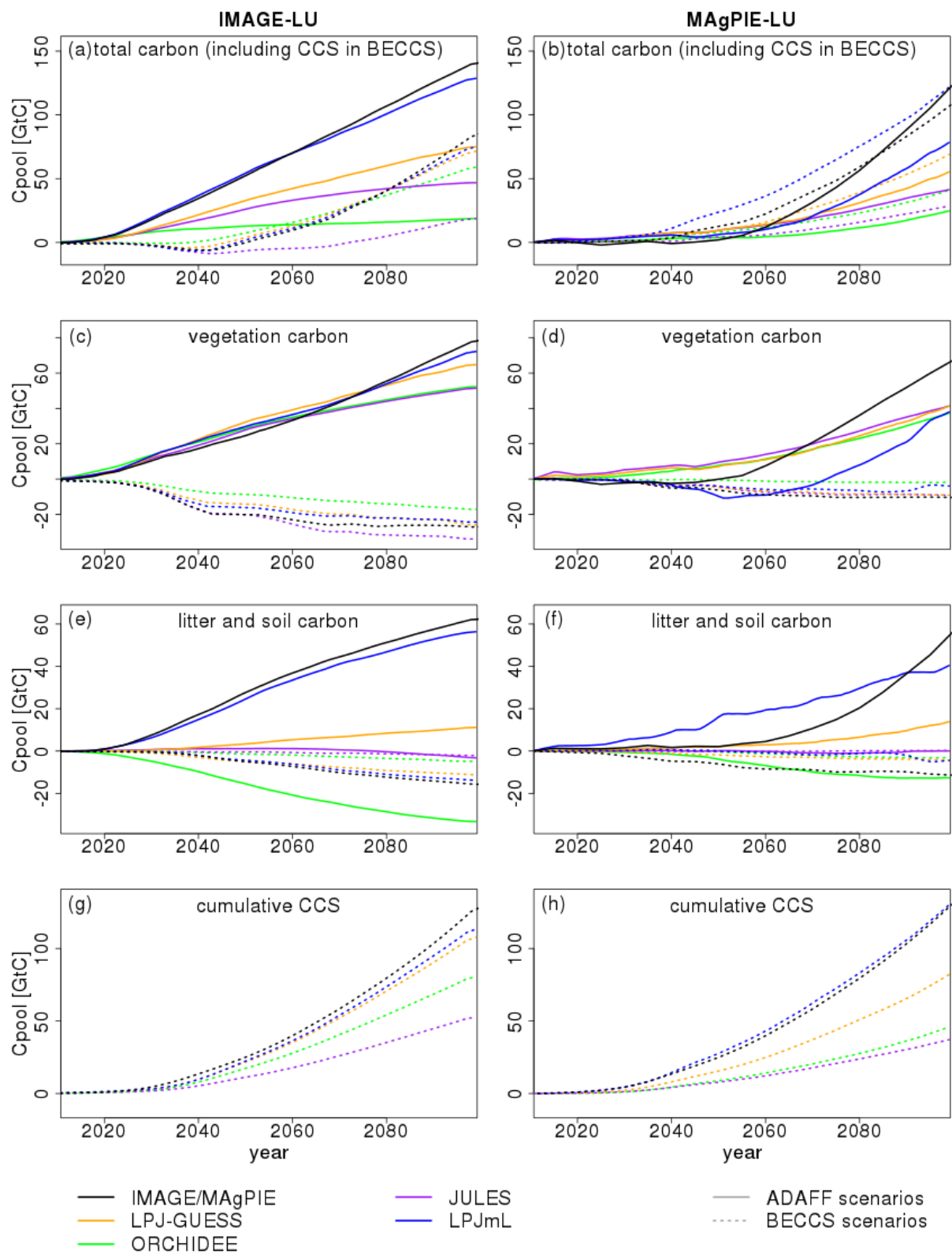LPJ-GUESS   LPJmL   BECCS scenarios
ORCHIDEE

Figure 1: Time-series (2010-2099) of simulated C uptake (total of all grid-cells) in the LUMs

and DGVMs for the mitigation simulations (compared to the respective BASE simulation),

for IMAGE-LU patterns (left, 5-year running means) and MAgPIE-LU patterns (right). a+b)

total C (including cumulative CCS), c+d) vegetation C, e+f) litter and soil C, g+h) cumulative
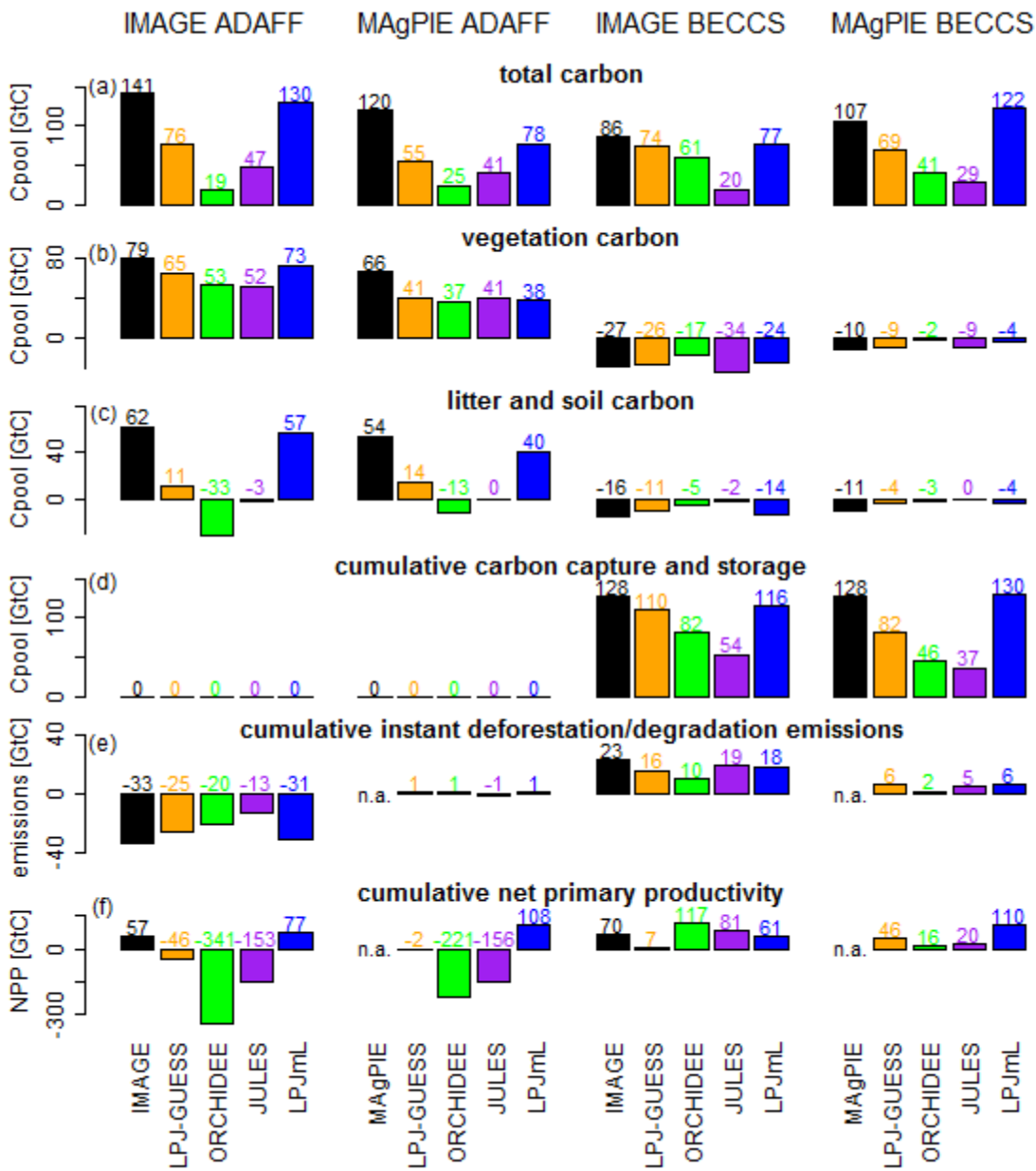
CCS.

836　Figure 2: Simulated change in total C (a), vegetation C (b), litter and soil C (c), cumulative

837　CCS (d), cumulative instant (oxidized in the same year) deforestation/degradation emissions

838　(e), and cumulative NPP (f) between year 2005 and 2099 for the mitigation simulations

839　(compared to the respective BASE simulation) in IMAGE/MAgPIE (as simulated by the

840　LUMs in the LUC scenarios), LPJ-GUESS, ORCHIDEE, JULES and LPJmL.
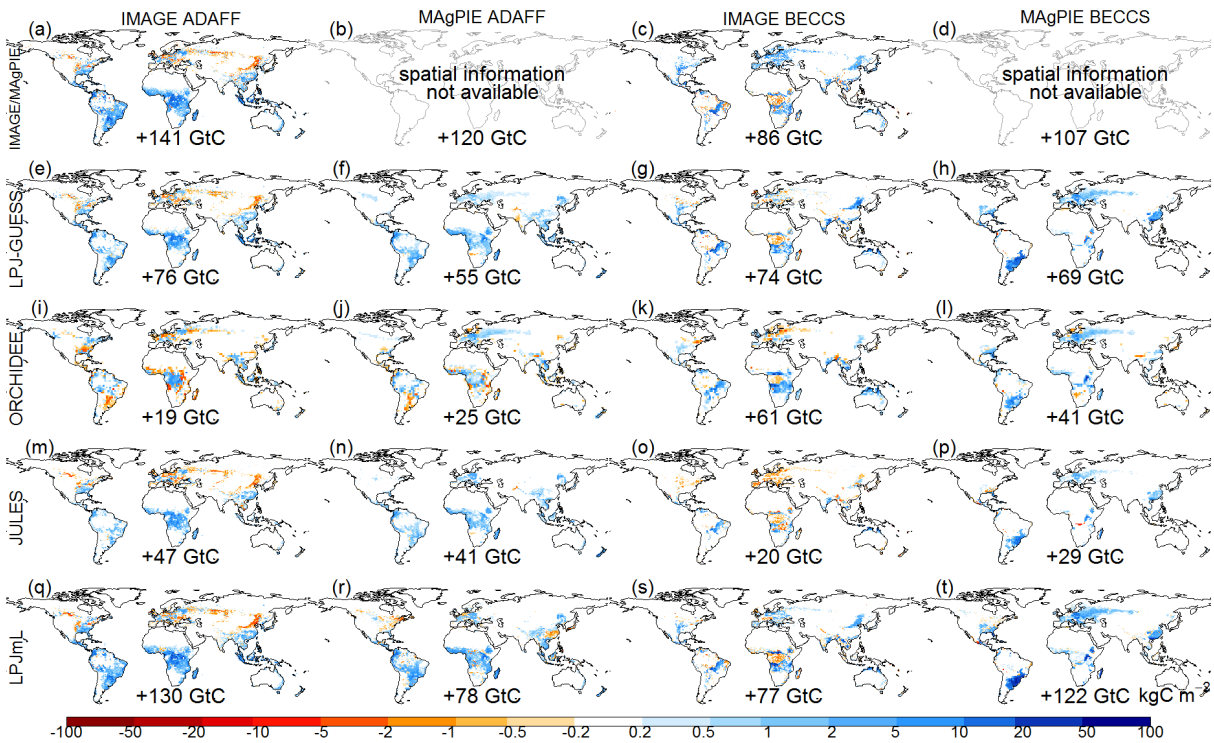
841

843　Figure 3: Spatial distribution of total C uptake in the LUMs (a-d) and DGVMs (e-t) for the

844　mitigation scenarios (compared to BASE) between year 2005 and 2099 for IMAGE ADAFF

845　(1st column), MAgPIE ADAFF (2nd column), IMAGE BECCS (3rd column) and MAgPIE

846　BECCS (4th column). Numbers are global totals.

847

848